

Corroles

Ligand Non-innocence and Single Molecular Spintronic Properties of Ag^{II} Dibenzocorrole Radical on Ag(111)Jialiang Xu[†], Li Zhu[†], Hu Gao, Chenhong Li, Meng-Jiao Zhu, Zhen-Yu Jia, Xin-Yang Zhu, Yue Zhao, Shao-Chun Li,* Fan Wu,* and Zhen Shen*

Abstract: A facile method for the quantitative preparation of silver dibenzo-fused corrole Ag-I is described. In contrast to the saddle conformation resolved by single-crystal X-ray analysis for Ag-I, it adopts an unprecedented domed geometry, with up and down orientations, when adsorbed on an Ag(111) surface. Sharp Kondo resonances near Fermi level, both at the corrole ligand and the silver center were observed by cryogenic STM, with relatively high Kondo temperature (172 K), providing evidence for a non-innocent Ag^{II}-corrole²⁻ species. Further investigation validates that benzene ring fusion and molecule-substrate interactions play pivotal roles in enhancing Ag(4d-(x²-y²))-corrole (π) orbital interactions, thereby stabilizing the open-shell singlet Ag^{II}-corrole²⁻ on Ag(111) surface. Moreover, this strategy used for constructing metal-free benzene-ring fused corrole ligand gives rise to inspiration of designing novel metal-corrole compound for multichannel molecular spintronics devices.

Spintronics^[1] is a novel technique that uses the electron spin and magnetic moment to construct new electronic devices rather than traditional electron charge, bringing great improvements in heat dissipation, power consumption, and speed. Traditional spintronics research mainly focuses on transition metals and inorganic semiconductors, while the advantage of organic molecules is that their electronic structures and magnetic properties are relatively easy to achieve effective spin control by changing the special external conditions. Advances in molecular spintronics with multiple

spin relaxation channels nowadays are highly desirable for fabricating ultrafast miniaturized data storage devices and logic gates.^[2] Scanning tunnelling microscopy (STM) has been demonstrated to be a powerful tool for studying spintronics through investigating the interactions between the unpaired molecular spins and the conduction band electrons of the substrate.^[3] Recent studies have shown that metal complexes of porphyrins^[4] and their analogues^[5] efficiently couple their delocalized unpaired π -electrons with the conduction band electrons of the metal substrate thus been extensively studied for molecular spintronics applications.^[6] As a representative branch of porphyrins, corrole can be viewed as a ring-contracted porphyrinoid containing direct pyrrole-pyrrole linkages and with the trianionic characteristics of the macrocyclic ligand. Corroles show remarkable coordination ability^[7] and chemical activities, which is widely used in the fields of catalysts,^[8] chemical sensors,^[9] solar cells^[10] and pharmaceutical manufacturing.^[11] Furthermore, by adjusting the HOMO orbital energy of corrole molecule, the regulation of the electron state could be easily achieved thus make it a promising candidate in spintronics.

Non-innocent ligands as special properties arising from d- π interaction^[12] are widespread among metallocorroles, especially among coinage metal corroles. Previous studies have shown that copper corroles are non-innocent,^[13] while gold corroles are innocent,^[14] depending on the metal (d_{x²-y²})-corrole(π) orbital interactions. However, describing silver corroles^[15] as innocent or non-innocent is very challenging. The crystal structures of silver triarylcorroles are mildly saddled, suggesting the existence of some degree of metal(d_{x²-y²})-corrole(π) orbital interactions in the silver case, which is less than that of copper but more than that of gold. Ghosh et al. reported a non-innocent silver β -octabromo-meso-triarylcorrole^[15d] based on its strongly saddled structure and Soret maxima being sensitive to the nature of the *para*-substituent, while a series of β -arylethynyl-substituted silver corrole complexes are proved innocent.^[15e] Therefore, studying the intriguing subtle properties of silver corroles in single molecular spintronics become attractive. Previously, we reported a planar triplet ground-state Cu^{II} tetrabenzocorrole with four fused benzene rings on the corrole ligand.^[5c] However, fused-ring expansions with other metal centers have rarely been studied in detail in terms of the interactions between metal centers and structurally modifying the corrole ligands and their spintronic properties, since it is difficult to remove the central copper ion or directly synthesize a free-base tetrabenzocorrole ligand.

Here, we described a novel dibenzo-fused silver corrole **Ag-1**, prepared by the facile retro-Diels-Alder reaction of

[*] J. L. Xu,^[†] H. Gao, C. H. Li, Dr. M. J. Zhu, Dr. Y. Zhao, Dr. F. Wu, Prof. Dr. Z. Shen

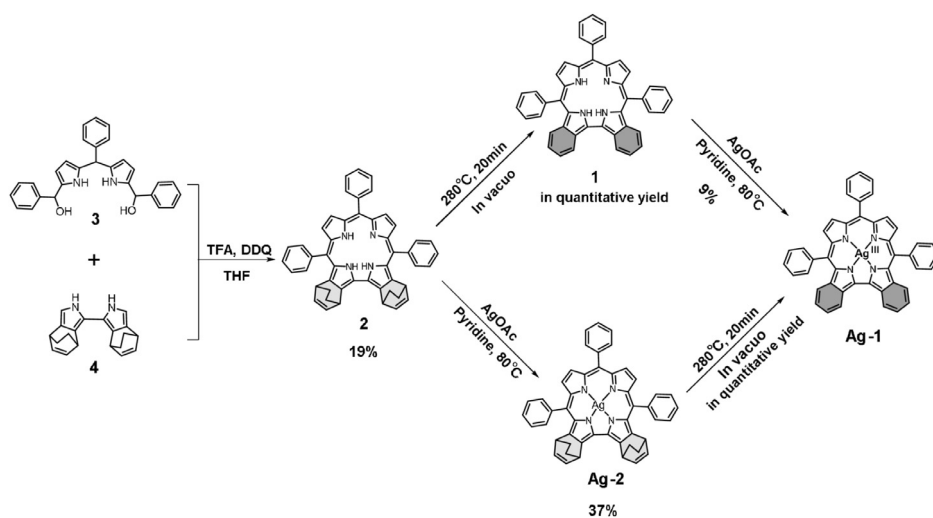
State Key Laboratory of Coordination Chemistry, Collaborative Innovation Center of Advanced Microstructures
Collaborative Innovation Center of Chemistry for Life Sciences
School of Chemistry and Chemical Engineering
Nanjing University, Nanjing 210046 (P. R. China)
E-mail: wufan@nju.edu.cn
zshen@nju.edu.cn

L. Zhu,^[†] Dr. Z. Y. Jia, X. Y. Zhu, Prof. Dr. S. C. Li
National Laboratory of Solid State Microstructures
School of Physics, Collaborative Innovation Center of
Advanced Microstructures, Nanjing University
Nanjing 210093 (P. R. China)
E-mail: scli@nju.edu.cn

Prof. Dr. S. C. Li
Jiangsu Provincial Key Laboratory for Nanotechnology
Nanjing University, Nanjing 210093 (China)

[†] These authors contributed equally to this work.

Supporting information and the ORCID identification number(s) for the author(s) of this article can be found under:
<https://doi.org/10.1002/anie.202016674>.



Scheme 1. Synthesis of dibenzo-fused silver corrole **Ag-1**.

a peripheral bicyclo[2.2.2]octadiene-fused (BCOD-fused) corrole **Ag-2**. The latter compound **Ag-2** was prepared through a [2+2]-type condensation reaction, followed by complexation with silver acetate (Scheme 1). **Ag-1** adsorbed on Ag(111) substrate was an open-shell singlet Ag^{II} -corrole $^{2-}$ state, which was found to adopt rare domed geometries that are significantly different from the normal saddle configuration resolved by single crystal X-ray analysis. In both domed geometries, Kondo effects were observed at the center metal as well as the ligand. Therefore, our research indicates that by stabilizing the unpaired electrons of metal and the π radical in the ligand provide a new pathway for developing multi-channel molecular spintronics devices for data storage and logic gates.

Other than copper corroles, research on fused-ring-expanded metal corroles has not been reported due to difficulties associated with their synthesis and purification. Through a facile method, fused-ring-expanded free-base corroles and the corresponding metalcorroles were successfully synthesized (Scheme 1). First, 2,17-dibicyclo[2.2.2]octadiene-fused corrole **2** was synthesized by the [2+2] condensation reaction of the 1,9-bis(phenyl)-5-phenyl-dipyromethane **3** and 1,1'-bis(4,7-dihydro-4,7-ethano-2H-indole) **4** (Supporting Information, Scheme S1). Complexation of **2** with silver acetate in pyridine yielded the 2,17-dibicyclo[2.2.2]octadiene-fused silver corrole **Ag-2**, which was converted into the 2,17-dibenzo-fused silver corrole **Ag-1** in quantitative yield by heating at 280°C under vacuum. Another approach to synthesizing **Ag-1** involves first preparing the 2,17-dibenzo-fused corrole free base **1** by the retro-Diels–Alder reaction of **2**, followed by metal coordination; however, **1** is relatively unstable in the air as well as the yield in the metal complexation step is poor (Scheme 1). The structures of the new macrocyclic products **1**, **2** and their silver complexes were characterized using various spectroscopic means (Supporting Information). This method can also be used to synthesize other fused-ring-expanded metalcorroles.

The molecular structures of free-base corrole **1** and its silver complex **Ag-1** were unambiguously determined by X-ray crystallography analysis. Single crystals of **1** and **Ag-1** were obtained by slow diffusion of *n*-hexane into a toluene solution or recrystallization from a mixture of toluene and methanol, respectively. The explicit crystal structures are shown in Figure 1, with crystallographic data listed in the Supporting Information, Table S1 and Figures S10, S11. The average silver-nitrogen (Ag–N) distances and the saddling dihedral angles of various silver corroles (Supporting Information, Figure S1) are summarized

in the Supporting Information, Table S2. **Ag-1** adopts mild saddle configuration. The Ag–N distances in **Ag-1** (1.958 Å, 1.970 Å) are slightly longer than those of the β -unsubstituted silver triarylcorroles, such as **Ag(TpFPC)**^[14] (1.943 Å, 1.963 Å) and **Ag(TpMePC)**^[15a] (1.948 Å, 1.960 Å), but smaller than those of the silver-octabromo-*meso*-triarylcorrole, for example, **Ag(Br₈TpMePC)** (1.983 Å, 1.983 Å). However, the average value of torsion angles (χ_1 – χ_3 , defined in Table S2, 31.1°) of **Ag-1** are smaller than those of **Ag(TpFPC)** (32.5°), **Ag(TpMePC)** (33.8°) and **Ag(Br₈TpMePC)** (59.0°). In addition, the mean plane deviation (m.p.d., defined by 23 core atoms in Table S2) of **Ag-1** (0.175 Å) is the smallest among the reported silver corroles. As well as the average value of dihedral angles between the three *meso*-aryl rings and the mean plane (Figure 1 c, 57.5° on average) of **Ag-1** are larger than those of other silver corroles. These phenomena declare the better planarity of **Ag-1** than those reported silver corroles.

To further illustrate the electronic states of **Ag-1**, an isolated single **Ag-1** molecule on Ag(111) has been characterized by STM; experimental details are available in the

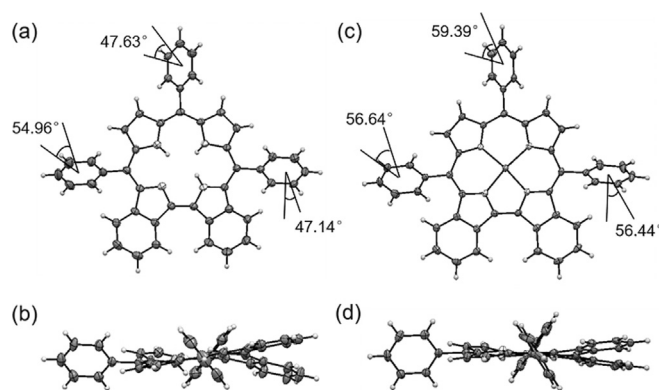


Figure 1. Top (up) and side (bottom) views of the X-ray crystal structures of **1** (a, b) and **Ag-1** (c, d) are shown with thermal ellipsoids at 50% probability.^[22]

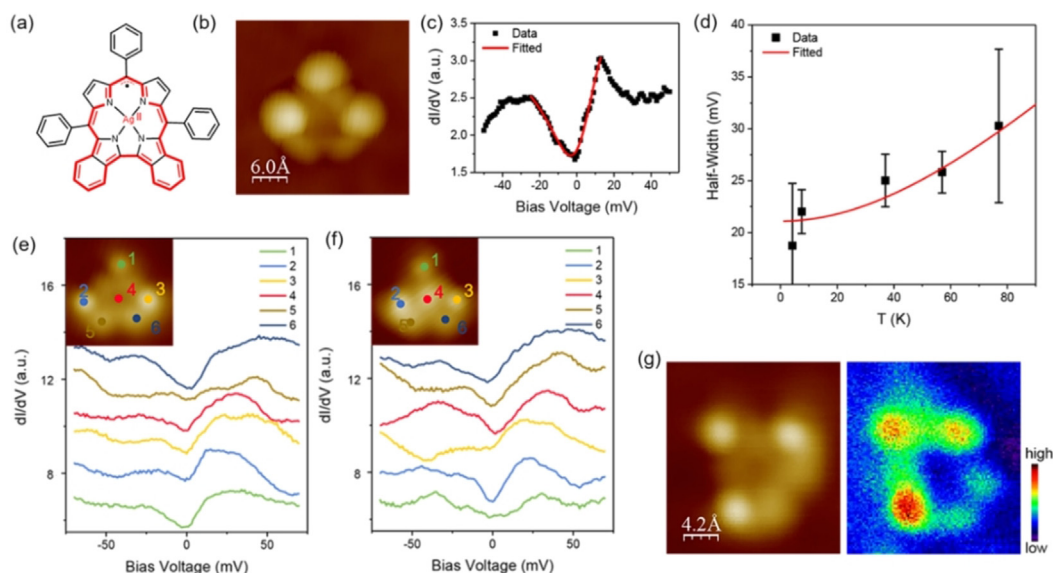


Figure 2. a) Molecular structure of **Ag-1**. b) STM image of a single **Ag-1** molecule (size: $3 \times 4 \text{ nm}^2$, $U = +200 \text{ mV}$, $I_t = 50 \text{ pA}$). c) dI/dV spectra of the **Ag-1** molecule ($U = +100 \text{ mV}$, $I_t = 200 \text{ pA}$, $U_{\text{mod}} = 2 \text{ mV}$). The red solid line is the fitted result using the Fano function. d) The half-width from the dI/dV spectrum of **Ag-1** on the Ag (111) film as a function of temperature and the fitted result. The error bars represent measurement deviations from different molecules. (e, f) Differential conductance dI/dV spectra ($U = +100 \text{ mV}$, $I_t = 200 \text{ pA}$, $U_{\text{mod}} = 2 \text{ mV}$) of six different characteristic sites of the two forms of **Ag-1** whose centers are hollow (inset of (e)) and protruded (inset of (f)). g) Morphological image of an **Ag-1** molecule and its dI/dV map in the vicinity of the Fermi level ($4 \times 4 \text{ nm}^2$, $U = +100 \text{ mV}$, $I_t = 200 \text{ pA}$, $U_{\text{mod}} = 10 \text{ mV}$).

Supporting Information. The **Ag-2** precursor was thermally sublimed onto an Ag(111) substrate in an ultra-high vacuum (base pressure of 1×10^{-10} mbar).^[16] During the sublimation process, **Ag-2** was converted into **Ag-1** by a retro-Diels–Alder reaction. The high-resolution STM topographical image (Figure 2b) of a single molecule adsorbed on the Ag(111) surface shows three bright bumps along with a ladder-shaped tail, which matches the molecular structure of **Ag-1** (Figure 2a).

However, **Ag-1** appears to adopt an unprecedented “dome-like” configuration, rather than the usual “saddle-like” configuration determined by X-ray crystallography. A previous report indicated that substrate-molecule interactions can change the configuration of a molecule adsorbed on a substrate surface.^[5c] In contrast to our previously reported copper tetrabenzocorrole, we observed both a protruded spot and a hollow area at the location of the central Ag atom in the STM map of **Ag-1**. Most of the **Ag-1** population adsorbed on the Ag(111) surface adopts the “Ag-Down” configuration, in which the central Ag is close to the substrate. As shown in the inset of Figure 2e, a slight depression is observed at the center of the “Ag-Down” configuration. On the other hand, the “Ag-Up” configuration, in which the central Ag is positioned away from the substrate, is only occasionally observed. The “Ag-Up” configuration exhibits a protrusion at the molecular center (inset of Figure 2f). These inequivalent populations may be due to the different formation energies of **Ag-1** on the Ag(111) substrate, and is easily understood in terms of the coupling of the central Ag ion to the Ag substrate, which lowers the formation energy; hence the central Ag ion in **Ag-1** tends to approach the substrate to increase molecule-substrate coupling.

The Kondo effect can be induced by the exchange between the spin of a delocalized π -radical and the conduction electrons of the substrate.^[17] Kondo resonance usually features a peak, dip, or kink near the Fermi energy in the STS spectrum,^[18] and is useful for investigating the spin state of a molecule. Figure 2c shows the differential conductance (dI/dV) spectrum taken at the center of the **Ag-1** molecule. A dip near E_F is evident in Figure 2c; this resonance feature was fitted to the Fano resonance function:^[19]

$$\frac{dI(V)}{d(V)} \propto \frac{(\varepsilon + q)^2}{1 + \varepsilon^2} \quad (1)$$

where $\varepsilon = (eV - \varepsilon_0)/\Gamma$, ε_0 is the energy shift from E_F , Γ is the full width at half maximum (FWHM) of the Fano resonance, and q is the Fano line-shape parameter. The good fit shown in Figure 2c suggests that the observed resonance is due to the Kondo effect of the **Ag-1** molecule. The Γ values obtained at various temperatures (T) are plotted in Figure 2d and are well described by the formula: $\Gamma = 2\sqrt{\pi k_B T^2 + 2(k_B T_k)^2}$ according to Fermi liquid theory.^[17c] The Kondo temperature T_k was determined to be about 172 K.

Notably, Kondo resonance is identified throughout the entire ligand (including the three *meso*-aryl rings 1–3 and the two fused benzene rings 5, 6) as well as the central Ag ion (4), as shown in Figure 2e. This is in sharp contrast to the previously studied Cu-tetrabenzocorrole,^[5c] which showed a Kondo effect only on the corrole macrocycle. As shown in Figure 2g, the topographical image and the dI/dV map of the **Ag-1** molecule show that the Ag center has the least of differential conductance, with larger ones appearing at the surrounding ligands, implying that resonance at the silver

center is most prominent, while that at the ligands is somewhat weaker. Kondo resonance was also observed on the occasional “Ag-Up” configuration, as shown in Figure 2 f, with similar results obtained.

DFT calculations using the VASP code with a plane-wave basis set were used to better understand the experimental results of STM; details can be found in the Supporting Information. Geometry optimization resulted in the open-shell singlet **Ag-1** on Ag(111) substrate adopting two differently oriented dome configurations (Figures 3 a–d). These calculation results are in good agreement with the experimental structures that we refer to as the “Ag-Down” and “Ag-Up” configurations. The distances between the molecule and the silver substrate are 2.775 Å for “Ag-Down” and 3.721 Å for “Ag-Up”. Meanwhile, the lengths of Ag–N bond are 1.996 Å and 2.010 Å for “Ag-Down”, as for “Ag-Up” is 1.983 Å and 1.985 Å (Supporting Information, Table S3). These bond lengths are much longer than those observed in the crystal structure of **Ag-1** and are closer to those of Ag^{II} porphyrins.^[20]

Three electronic states, namely the closed-shell singlet Ag^{III}-corrole³⁻, the open-shell singlet Ag^{II}-corrole²⁻, and the open-shell triplet Ag^{II}-corrole²⁻ radical were evaluated for **Ag-1** adsorbed on the Ag(111) substrate. The results listed in the Supporting Information, Table S4 revealed that the open-shell singlet state was the optimal ground state of **Ag-1** in the

“Ag-Down” configuration, the same conclusion could be drawn for the “Ag-Up” configuration. In addition, the ground state energy of the “Ag-Down” configuration was 9.489 kcal mol⁻¹ lower than that of the “Ag-Up” configuration, which quantitatively explains the dominance of the “Ag-Down” configuration in terms of the distribution of adsorbed molecules.

The spin-polarized partial density of states (PDOS) spectrum of the Ag atoms in the differently oriented **Ag-1** molecules in the absorption system (Figure 3 e) are predictably asymmetric. The peaks near the Fermi level that appear in the spectra of both configurations provide a theoretical possibility for observing the Kondo resonances in their scanning tunneling spectra.^[5a,b,21] The same conclusion can be drawn from the two calculated spin density plots as well (Figure 3 f for “Ag-Down” and Figure 3 g for “Ag-Up”). The lack of orthogonality between the three *meso*-aryl groups and the mean plane (the averaged dihedral angles is 51.1° for “Ag-Down” and 45.3° for “Ag-Up”) leads to the spin densities distribution over almost the entire molecule, even onto the *meso*-aryl groups, which is consistent with the Kondo resonances results observed at the 1–3 sites. These properties are obviously different from those of open-shell triplet tetraphenylconjugated copper with plane configuration.^[5c] Combined with the Bader valences of the central Ag ion results, with values of +1.76 determined for the “Ag-Down” and +1.83 for “Ag-Up” configurations, we conclude that the electronic state of **Ag-1** adsorbed on the Ag(111) surface is an open-shell singlet Ag^{II}-dibenzocorrole²⁻.

In summary, a novel free-base fused-ring-expansion corrole and its silver complex (**Ag-1**) were successfully synthesized for the first time. The electronic state of **Ag-1** on the Ag(111) substrate was studied by STM. Notably, two unprecedented “dome-like” configurations (“Ag-Down” and “Ag-Up”) are formed on the Ag(111) substrate. Obvious Kondo resonances near Fermi level, both at the corrole ligand and the silver center, were observed by STM, with a relatively high Kondo temperature (172 K). DFT calculations using the VASP code with a plane-wave basis set show that **Ag-1** behaves as an open shell singlet Ag^{II}-corrole²⁻ when adsorbed on the Ag(111) substrate. This is the first direct spectroscopic observation of the existence of Ag^{II} corrole radical. Meanwhile, this facile syntheses of the free-base and silver dibenzocorrole complex provides a new approach to the fine-tuning of interactions between the metal center and the corrole ligand. Stabilization of the unpaired electrons of silver and the π radical in the ligand provides a new pathway for the design of multi-channel molecular spintronics devices for data storage and logic gates. Efforts to further stabilize non-innocent metallocorroles by fusion with naphthalene and anthracene rings are currently underway.

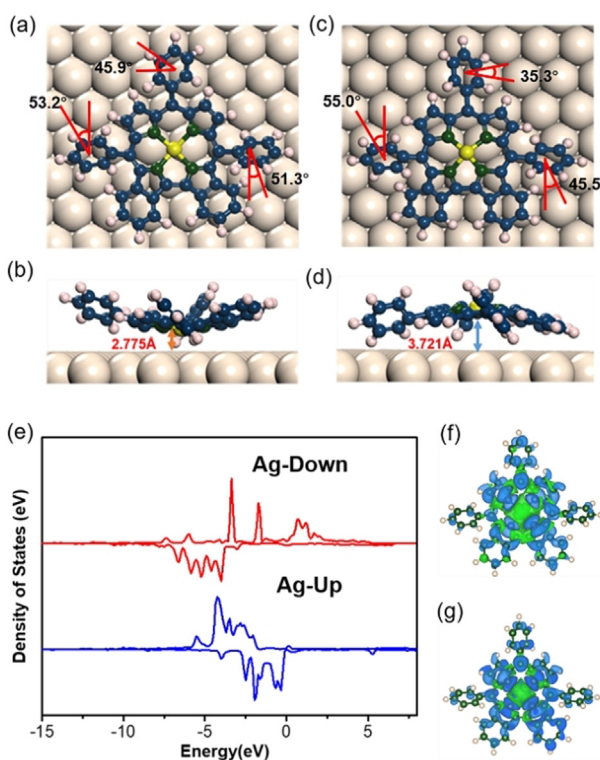


Figure 3. Top and side views of optimized geometries of the a, b) “Ag-Down” and c, d) “Ag-up” configurations in the adsorption system. The white balls represent the unit cell, which contains 46 Ag atoms per layer. e) Spin-polarized partial density of states (PDOS) spectra of the Ag atom in the “Ag-Down” (red) and “Ag-Up” (blue) configurations. The spin densities of the f) “Ag-Down” and g) “Ag-Up” configurations on the Ag(111) substrate.

Acknowledgements

This work was supported by the National Natural Science Foundation of China (Nos. 21771102, 22071103, and 21911540069) to Z.S., (No. 22001119) to F.W. and (Nos. 11774149, 11790311) to S.L.

Conflict of interest

The authors declare no conflict of interest.

Keywords: benzo-fused corroles · Kondo effect · non-innocence · silver corrole · spintronics

- [1] A. Cornia, P. Seneor, *Nat. Mater.* **2017**, *16*, 505–506.
- [2] a) J. Martínez-Blanco, C. Nacci, S. C. Erwin, K. Kanisawa, E. Locane, M. Thomas, F. von Oppen, P. W. Brouwer, S. Fölsch, *Nat. Phys.* **2015**, *11*, 640–644; b) D. Zou, W. Zhao, C. Yang, *Org. Electron.* **2019**, *69*, 120–127; c) X.-Y. Zhang, P. Zhao, *Phys. Lett. A* **2020**, *384*, 126256.
- [3] a) A. R. Rocha, V. M. García-Suárez, S. W. Bailey, C. J. Lambert, J. Ferrer, S. Sanvito, *Nat. Mater.* **2005**, *4*, 335–339; b) R. Requist, P. P. Baruselli, A. Smogunov, M. Fabrizio, S. Modesti, E. Tosatti, *Nat. Nanotechnol.* **2016**, *11*, 499–508; c) Z. Xu, J. Liu, S. Hou, Y. Wang, *Nanomaterials* **2020**, *10*, 2393.
- [4] a) J. Li, N. Merino-Díez, E. Carbonell-Sanromà, M. Vilas-Varela, D. G. de Oteyza, D. Peña, M. Corso, J. I. Pascual, *Sci. Adv.* **2018**, *4*, eaaq0582; b) A. DiLullo, S.-H. Chang, N. Baadji, K. Clark, J.-P. Klöckner, M.-H. Prosen, S. Sanvito, R. Wiesendanger, G. Hoffmann, S.-W. Hla, *Nano Lett.* **2012**, *12*, 3174–3179.
- [5] a) A. Zhao, Q. Li, L. Chen, H. Xiang, W. Wang, S. Pan, B. Wang, X. Xiao, J. Yang, J. G. Hou, Q. Zhu, *Science* **2005**, *309*, 1542; b) A. Mugarza, C. Krull, R. Robles, S. Stepanow, G. Ceballos, P. Gambardella, *Nat. Commun.* **2011**, *2*, 490; c) F. Wu, J. Liu, P. Mishra, T. Komeda, J. Mack, Y. Chang, N. Kobayashi, Z. Shen, *Nat. Commun.* **2015**, *6*, 7547.
- [6] a) R. Vincent, S. Klyatskaya, M. Ruben, W. Wernsdorfer, F. Balestro, *Nature* **2012**, *488*, 357–360; b) A. Candini, S. Klyatskaya, M. Ruben, W. Wernsdorfer, M. Affronte, *Nano Lett.* **2011**, *11*, 2634–2639.
- [7] a) S. Nardis, F. Mandoj, M. Stefanelli, R. Paolesse, *Coord. Chem. Rev.* **2019**, *388*, 360–405; b) A. Ghosh, *Chem. Rev.* **2017**, *117*, 3798–3881.
- [8] a) J. P. T. Zaragoza, M. A. Siegler, D. P. Goldberg, *J. Am. Chem. Soc.* **2018**, *140*, 4380–4390; b) M. Guo, Y.-M. Lee, R. Gupta, M. S. Seo, T. Ohta, H.-H. Wang, H.-Y. Liu, S. N. Dhuri, R. Sarangi, S. Fukuzumi, W. Nam, *J. Am. Chem. Soc.* **2017**, *139*, 15858–15867.
- [9] a) E. Jaworska, M. L. Naitana, E. Stelmach, G. Pomarico, M. Wojciechowski, E. Bulska, K. Maksymiuk, R. Paolesse, A. Michalska, *Anal. Chem.* **2017**, *89*, 7107–7114; b) B. Adinarayana, A. P. Thomas, P. Yadav, A. Kumar, A. Srinivasan, *Angew. Chem. Int. Ed.* **2016**, *55*, 969–973; *Angew. Chem.* **2016**, *128*, 981–985.
- [10] a) A. B. Alemayehu, N. U. Day, T. Mani, A. B. Rudine, K. E. Thomas, O. A. Gederas, S. A. Vinogradov, C. C. Wamser, A. Ghosh, *ACS Appl. Mater. Interfaces* **2016**, *8*, 18935–18942; b) R. Mishra, B. Basumatary, R. Singhal, G. D. Sharma, J. Sankar, *ACS Appl. Mater. Interfaces* **2018**, *10*, 31462–31471.
- [11] a) R. D. Teo, J. Y. Hwang, J. Termini, Z. Gross, H. B. Gray, *Chem. Rev.* **2017**, *117*, 2711–2729; b) Z. Zhang, H.-H. Wang, H.-J. Yu, Y.-Z. Xiong, H.-T. Zhang, L.-N. Ji, H.-Y. Liu, *Dalton Trans.* **2017**, *46*, 9481–9490; c) J.-M. Wang, Y. Li, H.-Q. Yuan, D.-H. Wu, X. Ying, L. Shi, H.-T. Zhang, H.-Y. Liu, *Appl. Organomet. Chem.* **2017**, *31*, e3571.
- [12] A. Ghosh, T. Wondimagegn, A. B. J. Parusel, *J. Am. Chem. Soc.* **2000**, *122*, 5100–5104.
- [13] a) S. Will, J. Lex, E. Vogel, H. Schmickler, J.-P. Gisselbrecht, C. Hauptmann, M. Bernard, M. Gorss, *Angew. Chem. Int. Ed. Engl.* **1997**, *36*, 357–361; *Angew. Chem.* **1997**, *109*, 367–371; b) A. B. Alemayehu, E. Gonzalez, L. K. Hansen, A. Ghosh, *Inorg. Chem.* **2009**, *48*, 7794–7799; c) C. M. Lemon, M. Huynh, A. G. Maher, B. L. Anderson, E. D. Bloch, D. C. Powers, D. G. Nocera, *Angew. Chem. Int. Ed.* **2016**, *55*, 2176–2180; *Angew. Chem.* **2016**, *128*, 2216–2220.
- [14] K. E. Thomas, A. B. Alemayehu, J. Conradie, C. Beavers, A. Ghosh, *Inorg. Chem.* **2011**, *50*, 12844–12851.
- [15] a) C. Brückner, C. A. Barta, R. P. Briñas, J. A. Krause Bauer, *Inorg. Chem.* **2003**, *42*, 1673–1680; b) M. Stefanelli, J. Shen, W. Zhu, M. Mastroianni, F. Mandoj, S. Nardis, Z. Ou, K. M. Kadish, F. R. Fronczek, K. M. Smith, R. Paolesse, *Inorg. Chem.* **2009**, *48*, 6879–6887; c) W. Sinha, M. G. Sommer, N. Deibel, F. Ehret, B. Sarkar, S. Kar, *Chem. Eur. J.* **2014**, *20*, 15920–15932; d) K. E. Thomas, H. Vazquez-Lima, Y. Fang, Y. Song, K. J. Gagnon, C. M. Beavers, K. M. Kadish, A. Ghosh, *Chem. Eur. J.* **2015**, *21*, 16839–16847; e) M. Stefanelli, A. Ricci, M. Chiarini, C. Lo Sterzo, B. Berionni Berna, G. Pomarico, F. Sabuzi, P. Galloni, F. R. Fronczek, K. M. Smith, L. Wang, Z. Ou, K. M. Kadish, R. Paolesse, *Dalton Trans.* **2019**, *48*, 13589–13598.
- [16] a) K. Katoh, Y. Yoshida, M. Yamashita, H. Miyasaka, B. K. Breedlove, T. Kajiwara, S. Takaishi, N. Ishikawa, H. Isshiki, Y. F. Zhang, T. Komeda, M. Yamagishi, J. Takeya, *J. Am. Chem. Soc.* **2009**, *131*, 9967–9976; b) T. Komeda, H. Isshiki, J. Liu, *Sci. Technol. Adv. Mater.* **2010**, *11*, 054602.
- [17] a) I. Fernández-Torrente, K. J. Franke, J. I. Pascual, *Phys. Rev. Lett.* **2008**, *101*, 217203; b) T. Komeda, H. Isshiki, J. Liu, Y.-F. Zhang, N. Lorente, K. Katoh, B. K. Breedlove, M. Yamashita, *Nat. Commun.* **2011**, *2*, 217; c) K. Nagaoka, T. Jamneala, M. Grobis, M. F. Crommie, *Phys. Rev. Lett.* **2002**, *88*, 077205.
- [18] U. Fano, *Phys. Rev.* **1961**, *124*, 1866–1878.
- [19] a) O. Újsághy, J. Kroha, L. Szunyogh, A. Zawadowski, *Phys. Rev. Lett.* **2000**, *85*, 2557–2560; b) M. Plihal, J. W. Gadzuk, *Phys. Rev. B* **2001**, *63*, 085404.
- [20] W. R. Scheidt, J. U. Mondal, C. W. Eigenbrot, A. Adler, L. J. Radonovich, J. L. Hoard, *Inorg. Chem.* **1986**, *25*, 795–799.
- [21] J. Liu, H. Isshiki, K. Katoh, T. Morita, B. K. Breedlove, M. Yamashita, T. Komeda, *J. Am. Chem. Soc.* **2013**, *135*, 651–658.
- [22] Deposition Numbers 2018948 (for **1**) and 1854807 (for **Ag-1**) contain the supplementary crystallographic data for this paper. These data are provided free of charge by the joint Cambridge Crystallographic Data Centre and Fachinformationszentrum Karlsruhe Access Structures service www.ccdc.cam.ac.uk/structures.

Manuscript received: December 19, 2020

Revised manuscript received: March 9, 2021

Accepted manuscript online: March 10, 2021

Version of record online: April 16, 2021